



Effect of diesel-palm biodiesel fuel with plastic pyrolysis oil and waste cooking biodiesel on tribological characteristics of lubricating oil



Muhamad Sharul Nizam Awang^{a,*}, Nurin Wahidah Mohd Zulkifli^{a,b,*},
Muhammad Mujtaba Abbas^{a,c}, Syahir Amzar Zulkifli^a, Md Abul Kalam^{a,b},
Mohd Nur Ashraf Mohd Yusoff^a, Wan Mohd Ashri Wan Daud^d,
Muhammad Hazwan Ahmad^e

^a Department of Mechanical Engineering, Faculty of Engineering, Universiti Malaya, 50603 Kuala Lumpur, Malaysia

^b Centre for Energy Sciences (CFES), Department of Mechanical Engineering, Faculty of Engineering, Universiti Malaya, 50603 Kuala Lumpur, Malaysia

^c Department of Mechanical, Mechatronics and Manufacturing Engineering (New Campus), University of Engineering and Technology Lahore, Lahore 54000, Pakistan

^d Department of Chemical Engineering, Faculty of Engineering, Universiti Malaya, 50603 Kuala Lumpur, Malaysia

^e Institute for Advanced Studies, Universiti Malaya, 50603 Kuala Lumpur, Malaysia

Received 29 September 2021; revised 14 December 2021; accepted 26 December 2021

Available online 04 January 2022

KEYWORDS

Plastic pyrolysis oil;
Waste cooking biodiesel;
Palm biodiesel;
Tribology;
Lubricant degradation;
Four ball

Abstract Engine oil's lubricity and tribological properties are changed when it is diluted with unburned fuels. SAE40 lubricating oil (LO) samples were contaminated with known percentage (5%) of fuels (commercial diesel (B10), diesel-palm biodiesel (PB) blend (B30a), and diesel-PB-plastic pyrolysis oil (PPO)-waste cooking biodiesel (WCB) blends (B20, B30b, and B40)). Utilizing -four-ball tester, the influence of each of these fuels on wear and frictional properties of LO was measured, and wear type on worn surfaces was examined. LO diluted by B10 had a high coefficient of friction (COF) (11.52%) with severe abrasive and adhesive wear than mineral lubricant followed by B30a (3.00%). LO mixed with quaternary fuels had a lower COF, wear scar diameter (WSD) and polishing wear. When compared to SAE40-B30a, SAE40-B30b had fewer frictional properties with adhesive wear. When compared to SAE-40 mineral lubricant, SAE40-B20 had the smallest increase in COF value (1.90%), followed by SAE40-B30b (2.17%), and SAE40-B40 (2.63%). While the WSD values for all tested samples are reduced by 3.12, 5.68, 6.33, 11.11, and 17.33%, respectively, when compared to pure lubricant for SAE40-B10, SAE40-B20, SAE40-B30a, SAE40-B30b, and

* Corresponding authors at: Department of Mechanical Engineering, Faculty of Engineering, Universiti Malaya, 50603 Kuala Lumpur, Malaysia (N.W.M. Zulkifli).

E-mail addresses: nizamawang95@gmail.com (M.S.N. Awang), nurinmz@um.edu.my (N.W.M. Zulkifli).

Peer review under responsibility of Faculty of Engineering, Alexandria University.

<https://doi.org/10.1016/j.aej.2021.12.062>

1110-0168 © 2021 THE AUTHORS. Published by Elsevier BV on behalf of Faculty of Engineering, Alexandria University.

This is an open access article under the CC BY-NC-ND license (<http://creativecommons.org/licenses/by-nc-nd/4.0/>).

Nomenclatures

B10	10% biodiesel and 90% diesel	GC-MS	Gas chromatography-mass spectrometry
B20	20% biodiesel and 80% diesel	HC	Hydrocarbon
B20a	80% diesel, 10% palm biodiesel, 5% plastic pyrolysis oil and 5% waste cooking biodiesel	LDPE	Low-density polyethylene
B30	30% biodiesel and 70% diesel	LO	Lubricating oil
B30a	70% diesel and 30% palm biodiesel	ME	Methyl ester
B30b	70% diesel, 10% palm biodiesel, 10% plastic pyrolysis oil and 10% waste cooking biodiesel	NaOH	Sodium hydroxide
B40	60% diesel, 10% palm biodiesel, 15% plastic pyrolysis oil and 15% waste cooking biodiesel	OM	Optical microscopy
CI	Compression ignition	PB	Palm biodiesel
CO	Carbon monoxide	PPO	Plastic pyrolysis oil
COF	Coefficient of friction	SEM	Scanning electron microscopy
FBT	Four-ball tester	WCB	Waste cooking biodiesel
		WCO	Waste cooking oil
		WSD	Wear scar diameter

SAE4-B40. PPO and WCB in B10 are found to reduce lubricant degradation when compared to diesel-PB blend and commercial diesel.

© 2021 THE AUTHORS. Published by Elsevier BV on behalf of Faculty of Engineering, Alexandria University. This is an open access article under the CC BY-NC-ND license (<http://creativecommons.org/licenses/by-nc-nd/4.0/>).

1. Introduction

Because of the depleting mineral reserves, global warming, and environmental issues, renewable, clean, and sustainable biofuels are becoming more significant [1]. In some parts of the world, up to 30% biodiesel in diesel is being utilized without any modifications to the diesel engine [2]. Currently, Malaysia and Indonesia have satisfactorily used B10, B20 and B30 diesel-palm biodiesel (PB) mixes, with Indonesia implementing B40 by 2022 [3,4]. By 2025, Malaysia is projected to have implemented B30 (30 % PB and 70% diesel) [5]. The use of a diesel-PB blend as a fuel reduced engine performance while improving exhaust gas emissions except for nitrogen oxides [6]. To improve the engine characteristics, several researchers utilized various alternative fuels (such as waste vegetable oil-based biodiesel and pyrolysis oil) in the diesel.

In pyrolysis oils, the diesel blend with plastic pyrolysis oil (PPO) outperformed the neat diesel in terms of engine performance and exhaust gas emissions [7,8]. PPO's brake-specific fuel consumption and brake thermal efficiency are both greater than diesel [7-9]. PPO produced less hydrocarbon (HC) emissions than diesel [10,11]. Whereas some researchers combined waste vegetable oil-based biodiesel with diesel as a substitute fuel to achieve better diesel engine performance while lowering emissions [12-14]. Sekhar et al. [15] reported that the addition of *Pithecellobium dulce* seed oil methyl ester (ME) in diesel improved engine performance and emission in terms of brake thermal efficiency and, carbon monoxide (CO) as hydrocarbon (HC), respectively. This trend of CO and HC emission is in line with the study conducted by Sekhar et al. [16]. Yatish et al. [17] reported the same trend of CO and HC emission, in which they were reduced by blending *Bauhinia variegata* biodiesel in diesel. Other studies also agreed that the addition of biodiesel in diesel improves diesel engine performance while lowering

emissions [18-21]. Waste cooking biodiesel (WCB) has also been identified as a viable alternative fuel for reducing engine exhaust gas emissions [22,23].

Some research investigated how biodiesel and diesel fuels affected the lubricating oil (LO) of compression ignition (CI) engines. According to Oakridge National Laboratory (USA), wear and friction account for around a quarter of the world's overall energy loss [24]. According to Agarwal [25], LO fuelled by 20% biodiesel system has less contaminants (such as soot, wear debris, oxidation products, resins, and moisture) and wear than a diesel-fuelled system. Because of biodiesel's self-lubricating properties, this was the case. Using high frequency reciprocating rig, Agarwal [25] investigated the influence of 10% B20 rapeseed oil biodiesel on the lubricity of a bio-lubricant (made from rapeseed oil). The results showed a reduced coefficient of friction (COF) and wear when contrasted to a synthetic lubricant mixed with 10% petroleum diesel.

Dhar and Agarwal [26] operated diesel engine for 200 h on diesel and B20 Karanja biodiesel fuel to examine the tribological properties of LO. LO comprised higher ash, wear trace metals, soot, and resins during biodiesel operation than throughout diesel operation. Because biodiesel (made from a variety of vegetable oils) and diesel have distinctive chemical compositions, their impacts on LO durability and degradation will be varied as well, as Agarwal [25] discovered. All corrosive and metallic wear debris was dissolved in the LO while the engine was operating. As a result, it is indeed critical to look into the influence of combustible fuels on lubricant tribology to see if they are suitable for CI engines.

In a research on LO degradation by biodiesel, Singh et al. [27] discovered that diluting B100 Moringa sp. ME in synthetic LO by 5-8% enhances lubricity, while increasing the dilution results in a higher wear rate. Other studies have observed sim-

ilar improvements in synthetic lubricant tribological properties after diluting with 5% biodiesel [28,29]. Meanwhile, Masjuki and Maleque [30] reported that more than 5 % PB in the lubricant caused oxidation and corrosion. The similar result was also reported by Awang et al. [31]. The addition of combustible fuel to the lubricant changed its lubricating properties and resulted in poor tribological performance. According to this issue, Mujtaba et al. [2] investigated the effects of alcoholic or nanoparticle additives on contaminated lubricant tribology in diesel-palm-sesame biodiesel. Nanoparticles in biodiesel blends (B30) were shown to be more effective at reducing lubricant degradation than alcoholic fuel additives and commercial diesel. Because of crankcase diluting during engine running, a–5% contamination of lubricant with fuels occurred [32].

There is a limited research on LO degradation by pyrolysis oil. Awang et al. [31] reported that mineral lubricant contaminated with blank PPO showed greater lubricant degradation compared to B10. Awang et al. [31] also studied the tribological behavior of LO deterioration using pyrolysis oil–biodiesel fuel. They found that adding 10 % PB in PPO reduces the lubricant degradation compared to blank PPO. However, with increasing PB content in the secondary contaminated samples, the COF increased. The same trend was also observed in their wear scar diameter (WSD). Different sources of biodiesel could be explored to find suitable biodiesel to be blended with PPO in order to reduce its lubricant degradation, especially at high concentration of biodiesel. In addition, no study has yet to be reported on the tribological behavior of LO deterioration using diesel–biodiesel–pyrolysis oil fuel.

Furthermore, a few researchers is apprehensive regarding LO deterioration caused by the blending of flammable fuels and lubricant during crankcase dilution. This research is the continuous work for authors' previous work [33]. In fact, PPO and WCB can be used in combination with PB-diesel blend as a quaternary fuel. They have a positive effect on improving the performance characteristics of diesel engines and reducing exhaust gas emissions. In addition, both fuels are promising alternative fuels in the B10 mixture, which in turn can enhance its lubricity. However, the contamination effect of these quaternary fuels in commercial lubricant is not reported. The change in engine oil characteristics is also not highlighted. It is necessary because engine longevity will be decreased as a result of diesel fuel contamination of the LO (mixed with biodiesel and pyrolysis oil).

In this investigation, diesel-PB fuels containing WCB and PPO were diluted with commercial LO up to 5% and were examined on how they influenced contaminated LO tribology. To the authors' knowledge, no one has looked at the tribology of contaminated lubricant using different diesel-PB-WCB-PPO mixtures. Only one research on the tribological effects of PPO and biodiesel-based fuel was published, and it only provided the change in COF over time, and average COF and WSD of contaminated lubricants [31]. It is insufficient to explain the contamination effects of these blends. Future study should study the wear characteristics on the worn metal surface. Therefore, this study focused on lubrication degradation caused by dilution using those quaternary blends in term of COF, WSD and worn metal surface, which had never been done previously. Using a four-ball tester (FBT), the influence of five different fuels on the tribological characteristics of LO was investigated (commercial diesel (B10), diesel-PB blend

(B30a), as well as B20a, B30b, and B40, which included diesel, PB, PPO, and WCB).

2. Materials and methods

2.1. Materials

KL-Kepong Oleomas Sdn Bhd provided the PB, while Syngas Sdn Bhd provided the PPO. A local restaurant's waste cooking oil (WCO) was collected. WCO was employed as a feedstock in the current study to prepare biodiesel. The local market provided 12.7 mm diameter AISI 52100 steel balls with a hardness of 64–66 Rc.

2.2. PPO production

Wastes made of low-density polyethylene (LDPE) were collected and processed into black pellets. The pyrolysis of LDPE black pellets in the absence of oxygen, catalytic reforming, and condensation of the resultant gases were used to convert them to PPO. The reactor was a semi-batch kind that could be moved around. When the LDPE black pellet was exposed to water vapour, it turned into molten plastic. The molten plastic was heated to a regulated temperature (500 °C) in the pyrolysis reactor. The vaporising pressure forced the gaseous product to pass through the catalytic chamber. The gaseous product was cracked even further in the catalytic chamber before being vented. Condensation and distillation of the gaseous product happened after passing through the chamber. The PPO condensate was then heaped up in the storage tank.

2.3. WCB production

The collected WCO was heated gradually up to 100 °C for 10 min to reduce the moisture content. The heated WCO was left until its temperature dropped to room temperature, then the filtration process was performed to remove solid particles. The transesterification was carried out in a glass reactor equipped with a heating jacket connected to a heated thermostat bath and fitted with a reflux condenser and mechanical stirrer. The 1000 mL WCO was first heated to 60 °C. Within this process, 90 g of methanol (30 wt% of WCO) and 3 g of sodium hydroxide (NaOH) (1 wt% of WCO) were mixed into a beaker. Next, the NaOH pellet was dissolved into the methanol and forming a meth oxide solution by using stirrer at 1100 rpm. The transesterification reaction was carried out by mixing 300 g of WCO and meth oxide solution by using mechanical stirrer (at 830 rpm) and heated at 60 °C for 1 h. After that, the product was placed in a separating funnel and left for 24 h. There were two distinct layers of biodiesel and glycerol found. The glycerol layer, which was on the bottom, was discarded. To obtain the pure biodiesel, the top layer of biodiesel was rinsed with warm water.

2.4. Samples preparation

2.4.1. Fuel sample preparation

To examine the lubricity and influence of quaternary fuel mixes on diesel engine parameters, several fuel samples were prepared. The produced fuel samples were compared to

Table 1 The composition of different tested quaternary fuel blends.

Sample	Fuel composition (by volume)
B10	90% diesel and 10 % PB
B30a	70% diesel and 30 % PB
B20a	80% diesel, 10 % PB, 5% PPO and 5% WCB
B30b	70% diesel, 10 % PB, 10% PPO and 10% WCB
B40	60% diesel, 10 % PB, 15% PPO and 15% WCB

Malaysian diesel that is commercially accessible (B10). To make the B30 fuel blend, PB was mixed with B10 diesel. 20 % PB was combined with 80% B10 diesel (by volume) and agitated for 30 min at 700 rpm until homogeneous. Additionally, three quaternary fuel blends were prepared as shown in Table 1. Fig. 1 shows the tested fuel blends.

2.4.2. Lubricant sample preparation

To begin, 5% of each of the fuels mentioned in Table 1 were combined with commercial SAE-40 lubricant using a magnetic stirrer at 900 rpm for 30 min, because the lubricant combination with the fuel was only 5% owing to crankcase dilution [34]. A viscometer (SVM 3000) was used to measure the physicochemical characteristics of SAE-40 reference lubricant and all other lubricant samples with various fuels, as indicated in Table 2.

2.5. Gas chromatography and mass spectrometry (GC–MS) analysis

As described in Table 3, the composition of binary fuels (B10 and B30a) and quaternary fuels (B20a, B30b and B40) was determined using GC–MS. After 50 mg of liquid fuel product was dissolved in 1 mL of n-hexane, the sample was put into the chromatographic inlet and processed for 42 min. The carrier gas is helium, which has a flow rate of 0.51 mL/min. The separation started at a temperature of 50 to 250 °C, with a heating rate of 5 °C/min [35].

2.6. Experimental set-up

2.6.1. FBT rig

A FBT (TE-800-FBT, Magnum Engineers, Bengaluru, India) was used to investigate the link between various fuels and their

impact on the tribological characteristics of lubricant, as shown in Fig. 3. To begin, a temperature sensor was attached to the cup holder, which held three stationary steel balls, and then 10 mL of the lubricant sample was added. Four fresh separated steel balls were utilised in each trial. All of the tests carried out in this study, which are in line with the standard test method ASTM D4172, were conducted under the working circumstances listed in Table 4. The experiments for each fuel sample were triplicated for assisting the constancy of measured values. These approaches were adapted from Mujtaba et al. [36].

Optical microscopy (OM) was used to determine the wear scar diameter (WSD) of worn steel ball after tribological studies. Eq. (1) and (2) below were used to calculate the WSD of worn surfaces and the COF:

$$\text{WSD} = \frac{M + N}{2} \quad (1)$$

where M is the main axis (μm) as measured by OM. N is the minor axis (μm) as measured by OM. Fig. 2 shows the measurement of M and N values of worn steel ball by using OM.

$$\text{COF} = \frac{\text{Actual frictional force (N)}}{\text{Applied Load (N)}} \quad (2)$$

2.7. Scanning electron microscopy (SEM) analysis

SEM was used to study the surface morphology of a worn steel ball after tribological testing. To visualise the type of wear, SEM pictures were taken at a magnification of 3000.

3. Results and discussion

3.1. Tribological characteristics of lubricant samples: COF and WSD

Fig. 4 shows the COF of all lubricant samples during the running-in and steady-state conditions. Fig. 4 also shows how the COF of all investigated samples increases dramatically at the start of the testing, known as the run-in phase. The running-in phase is defined as a series of processes that occur during which wear rates and friction for lubricated contacts stabilise. There was no lubricating coating between these metallic contact throughout the run-in phase, resulting in a drastic increment of COF about at first 5 min of each experiment, as shown in Fig. 4.

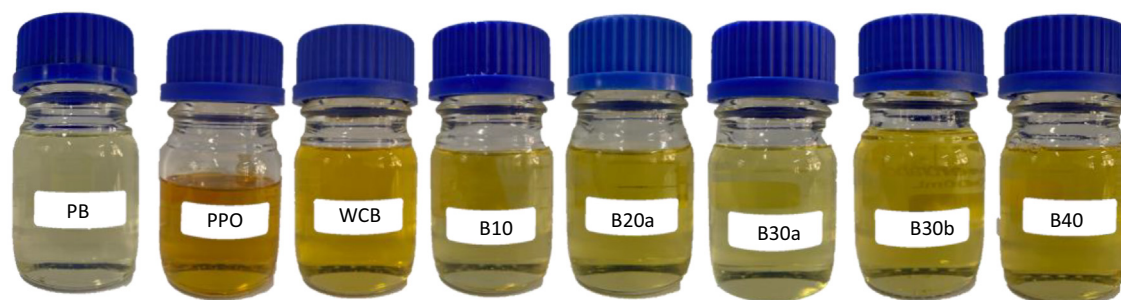
**Fig. 1** Tested blank fuels and quaternary fuel blends.

Table 2 Physicochemical properties of tested lubricant fuel samples.

Properties of test fuel	100% Lubricant (SAE 40)	SAE 40 + 5% POB	SAE40 + 5% B10	SAE 40 + 5% PPO	SAE 40 + 5% WCB	SAE 40 + 5% B20a	SAE 40 + 5% B30a	SAE 40 + 5% B30b	SAE 40 + 5% B40
Density at 15 °C (kg/m ³)	894.1	892.4	895.4	888.9	0.8932	891.0	891.7	891.2	891.3
Kinematic viscosity at 40 °C (mm ² /s)	129.63	98.15	129.44	85.943	94.409	94.631	95.608	93.272	93.002
Kinematic viscosity at 100 °C (mm ² /s)	13.33	11.56	11.62	10.799	11.283	11.526	11.315	11.357	11.203
Dynamic viscosity at 40 °C (mPa.s)	113.86	86.04	113.68	75.003	82.823	82.801	83.735	81.414	81.24
Dynamic viscosity at 100 °C (mPa.s)	11.21	9.70	9.73	9.0039	9.4673	9.6174	9.4775	9.4996	9.3785
Viscosity index	96.9	105.5	70.0	110.5	106.1	112.1	104.9	107.0	106.8

Table 3 Chemical composition of binary fuels (B10 and B30a) and quaternary fuels (B20a, B30b and B40).

Chemical composition		Amount (%)					
		B10	B20a	B30a	B30b	B40	
Carbon number range							
Alkane	C ₁ -C ₁₀	0.39	6.82	3.49	11.28	10.29	
	C ₁₁ -C ₂₀	43.72	31.99	53.66	22.17	43.85	
	C ₂₁ -C ₃₀	4.30	3.05	6.79	2.88	8.43	
	C ₃₁ -C ₄₀	2.32	6.69	2.82	1.04	1.48	
Alkene	C ₁ -C ₁₀	0.29	1.80	2.99	4.06	2.98	
	C ₁₁ -C ₂₀	–	–	0.58	4.01	2.51	
Benzene		4.94	11.99	7.78	7.37	8.90	
Naphthalene		4.03	10.60	10.92	6.53	8.6	
Fatty acid ME	Common name						
	Structure						
	Lauric acid ME	C12:0 ME	–	0.43	0.40	0.36	0.40
	Myristic Acid ME	C14:0 ME	0.80	0.62	1.17	0.53	0.56
	Palmitic acid ME	C16:0 ME	2.09	–	0.81	2.13	2.22
	Heptadecanoic acid ME	C17:0 ME	–	1.61	1.53	–	0.82
	Oleic acid ME	C18:1 ME	–	1.11	1.94	0.96	0.48
	Arachidic acid ME	C20:0 ME	0.43	0.48	–	0.56	0.65
Total saturated fatty acid ME		3.32	3.14	3.91	3.58	4.65	
Total unsaturated fatty acid ME		–	1.11	1.94	0.96	0.48	

The steady-state phase occurs when the fraction trend stabilises after a few minutes due to the formation of a protective lubricating layer between rubbing surfaces [2]. Lubricants with quaternary fuel dilution (SAE40-B20a, SAE40-B30b, and SAE40-B40) had less friction and were 8.90–9.62% lower than

lubricants contaminated with B10 (SAE40-B10). According to previous studies [37,38], biodiesel fuel diluted in LO produces less degradation, whereas PPO dilution in LO causes greater degradation [31].

In addition, compared to diesel-contaminated lubricant, adding WCB and PPO to B10 diesel increased lubricant lubricity and decreased COF. The presence of oxygenated moieties and an excess of oxygen in the chemical composition of WCB and PPO, a long-chain polymer-based oil, improved the overall lubricity of B10 + PPO + WCB-contaminated LO [2,37,38].

Fig. 5 shows the average COF of stationary and spinning balls, as well as the WSD of the examined steel balls. SAE-40 (SAE40), a 100% pure reference lubricant, had the lowest COF (0.1474). However, due of the decrease in viscosity, lubri-

Table 4 FBT operating conditions.

Test parameters	Standard value
Test duration	60 min
Applied load	40 kg
Oil temperature	75 °C
Rotational speed of spindle	1200 rpm

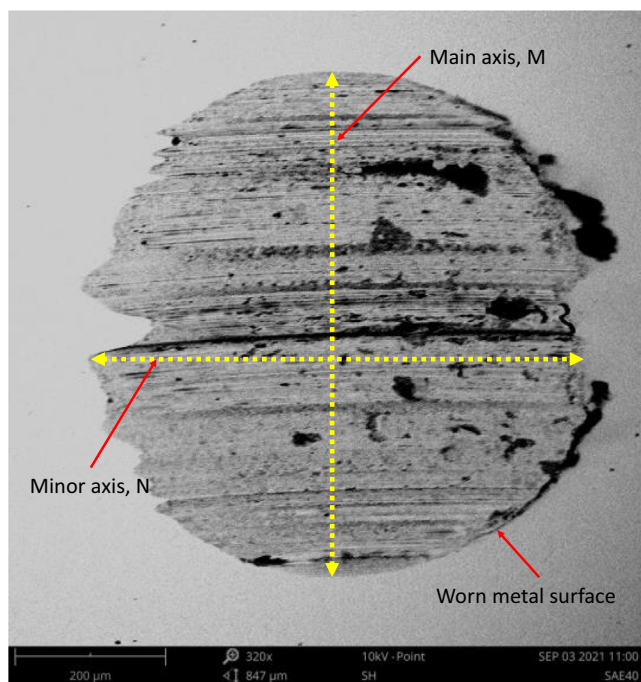


Fig. 2 Measurement of main axis, M and minor axis, N on worn metal surface by OM.

contaminated dispersion by fuels resulted in an increase in COF [2,31]. Lubricant contaminated with PB showed the highest COF (0.1680) than all other lubricant samples, followed by B10 (0.1654). The oxidation process turns the esters into various fatty acids, such as formic acid, acetic acid, propionic acid, caproic acid, and so on. Polyunsaturated fatty acid ME, such as oleic acid ME Table 3, are perhaps the most important factor regulating auto-oxidation in POB. Fuel degradation can

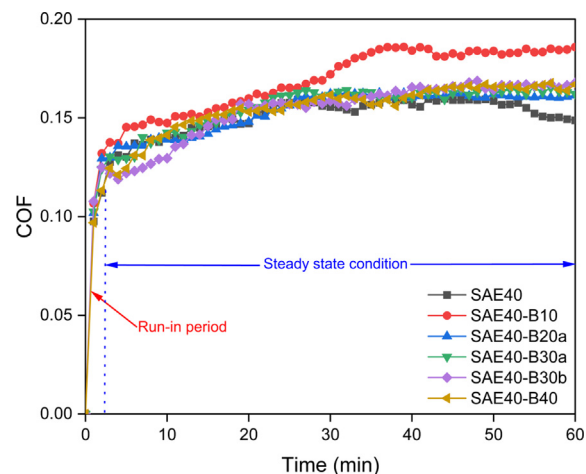


Fig. 4 COF trend for all tested samples with respect to time.

occur as a result of the oxidation process, resulting in decreased lubricity, increased corrosion, and material deterioration [31]. The COF of contaminated lubricants contaminated with quaternary fuels was substantially lower than those of PB and diesel fuel contaminated lubricants.

All contaminated lubricant fuel samples, SAE40-B10, SAE40-B30a, SAE40-40, SAE40-B30b, and SAE40-B20a, had greater COF than blank lubricant sample (SAE40) by 11.52, 3.00, 2.63, 2.17, and 1.90%, respectively. The action of carboxylic acids generated by biodiesel fuel degradation was thought to be the cause of the elevated COF [39]. Because of the high proportion of sulfur in B10 fuel, SAE40-B10 had a high COF (0.1654) and inferior lubricity of all the samples tested. Due to oxidation of the metallic surface, the high oxygen concentration of the B30a fuel sample resulted in significant wear and COF [30,31]. The COF of SAE40-B30b

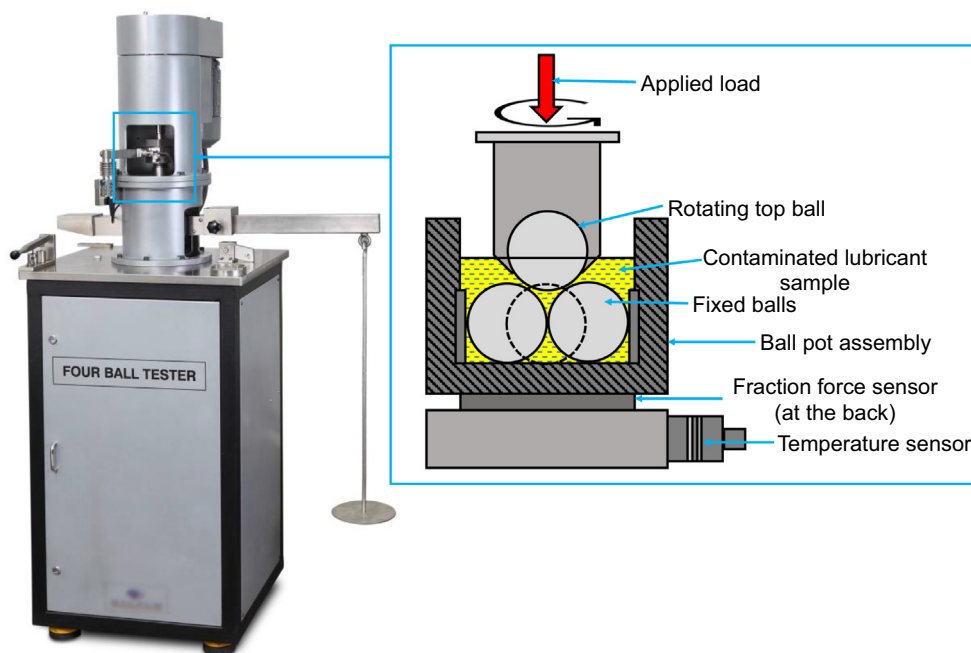


Fig. 3 Schematic view of FBT rig.

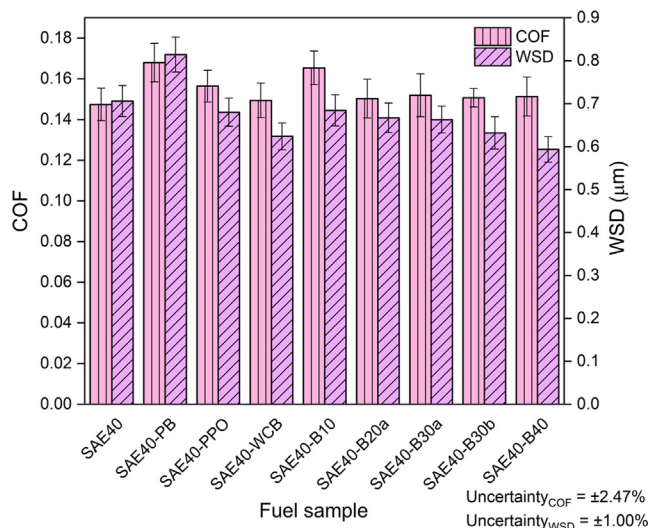


Fig. 5 Average COF and WSD of lubricant samples.

lubricant sample was 0.83% lower than a B30a contaminated lubricant sample and 9.35% lower than a diesel contaminated lubricant sample. B30b works as a friction-resisting agent in the lubricant sample, producing a protective barrier between the metallic contacts, since the ester compounds in biofuel and the long chain polymers in PPO operate as a ball bearing between rubbing surfaces [40,41]. Furthermore, the polar esters found in WCB can effectively reduce friction by deposit-

ing on the contact interface to produce a continuous, stable anti-friction layer, as reported by earlier study [42]. Under comparable operating conditions, the SAE40-B20a sample had the lowest friction coefficient of all the quaternary fuels. The lubricating layer stability between rubbing surfaces is affected by speed, applied load, fluid viscosity, fuel fatty acid ME content, and temperature [28].

Because of polarity-imparting oxygen atoms contained in the ME group of biodiesel that promotes lubricity, the WSD of SAE40 was significantly high, whereas dilution of lubricant with fuel samples lowered WSD. Other researchers explained the same reasoning [2,43,44]. When compared to blank lubricant and SAE40-B10, B10 with PB, PPO, and WCB showed lower WSD due to the ester molecule and long-chain polymer that act as a small ball bearing rolling between rubbing surfaces, leading to less wear [40,41].

SAE40-B30a showed a greater WSD value than SAE40-B30b due to oxidation products that dissolve the oxide coatings between metallic contact surfaces such as piston and cylinder, resulting in increased COF and wear. Due to the long carbon chain fatty acid ME and high proportion of unsaturated fatty acid ME, lubricant contaminated with B30a had a high WSD, as indicated in Table 3. Because of the ester molecule in the WCB, all quaternary fuel-contaminated fuels have a downward trend in WSD values. Among all quaternary fuel lubricants, the SAE40-B20a tested fuel had the highest WSD. The reduced kinematic viscosity of SAE40-B20a causes difficulty in establishing a protective layer between metallic surfaces, resulting in poor lubricity. In comparison to pure

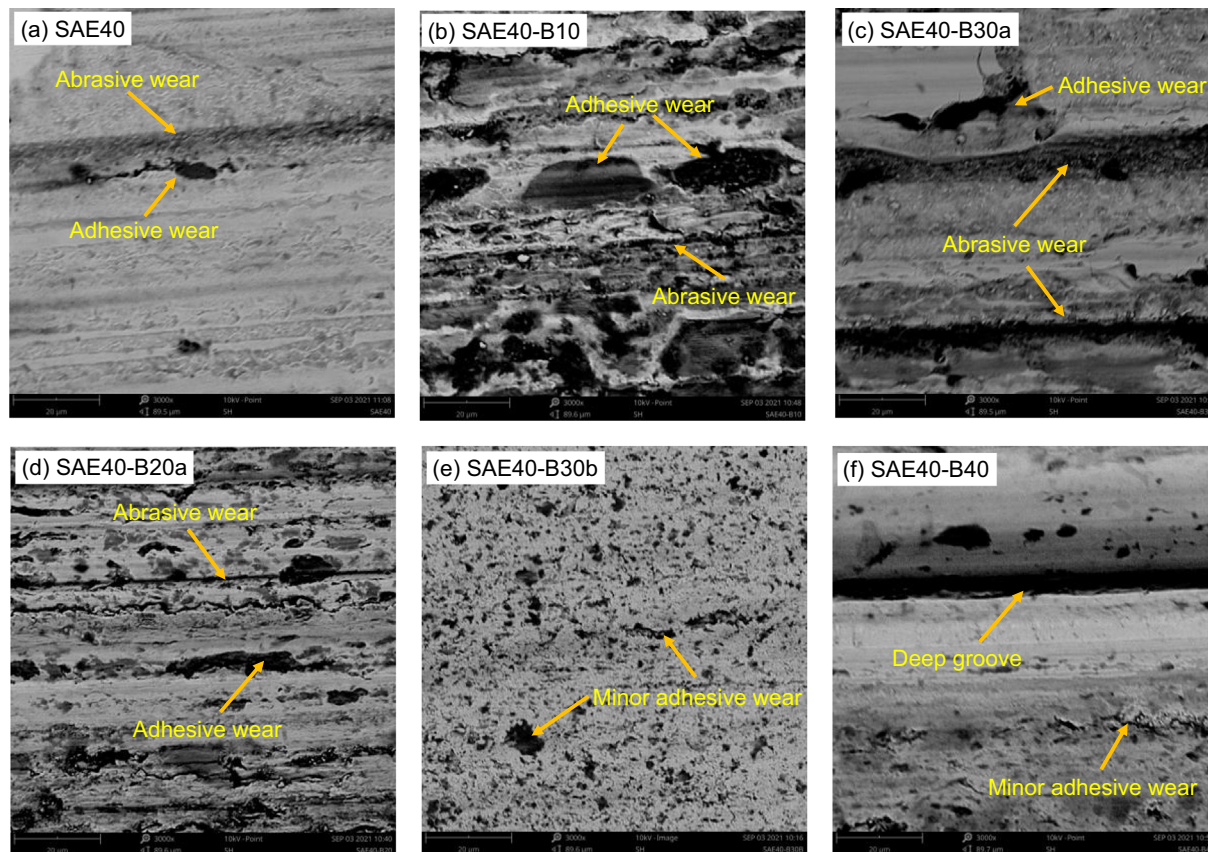


Fig. 6 Morphological images of worn steel ball by SEM.

lubricant, WSD values for SAE40-B10, SAE40-B20a, SAE40-B30a, SAE40-B30b, and SAE40-B40 are reduced by 3.12, 5.68, 6.33, 11.11, and 17.33%, respectively. The presence of ester molecules and oxygen concentration in biodiesel contribute to better wear characteristics, resulting in lower WSD [2].

3.2. Worn ball surface analysis by SEM

Fig. 6 shows morphological images of worn steel balls that were utilized to evaluate lubricant samples. Contamination of lubricant with B10 elevated its wear, as abrasive and adhesive wear were seen. When material expelled from the worn steel ball chamber of a lubricant contaminated with B10 is more than 20 μm , adhesive wear develops. Particles less than 20 μm in all assessed samples retrieved from worn steel ball cavities are classified as abrasive wear [2]. Scratches are the result of abrasive wear. Scratches can be found in SAE40-B10. This is owing to the COF's instability and the lack of a lubricating thin layer between mating metallic surfaces. Mujtaba et al. [2] also made the same observation. In LO, B30a biodiesel fuel exhibited less wear than diesel fuel. SAE40-B30a showed less wear than SAE4-B10 due to the large amount of oleic acids (as indicated in Table 3), which serves as a lubricity booster [45].

As a result of the chemical interaction of PPO on the steel ball surface to preserve the rubbing surface, polishing wear was seen in PPO-based quaternary fuel in lubricant [41]. It signifies that PPO is a chemically active alternative fuel that produces relatively smooth surfaces. Because chemically active films formed between rubbing surfaces, SAE40-B30b provided less wear than SAE40-B30a, as seen in Fig. 6. With deep grooves (abrasive wear) being apparent on the worn surface, SAE40-B40 demonstrated less wear than other quaternary fuel contaminated lubricants. When PPO and WCB were introduced to B10, friction and wear of LO were decreased due to the formation of a lubricating layer between rubbing surfaces.

3.3. Uncertainty analysis

Several factors might contribute to errors and uncertainties during an experiment, including calibration, observation, data collection procedures, test parameters, planning and design, etc. Uncertainty analysis is a method for validating experimental results. The uncertainties calculation for the tribological parameters are presented in the Appendix. The overall uncer-

tainty was determined using the following equation presented by How et al. [2]:

The overall uncertainty was then calculated using the following equation.

$$\text{Overall experimental uncertainty} = \sqrt{\sum (\text{Uncertainty of each parameter})^2}$$

4. Conclusion

Using a FBT according to the ASTM D4172, the influence of PPO and WCB in B10 on tribological parameters of LO (SAE-40) was studied in this study. Because of the high proportion of sulfur in B10 fuel, SAE40-B10 had a high COF (11.52%) and inferior lubricity among all studied samples. A substantial drop in the parameters, COF, and WSD was seen for lubricant contaminated with quaternary fuels, as well as other contaminated lubricant samples. Dilution of B30b fuel in LO produces less degradation than B30a. Due to oxidation products that erode the oxide coatings between metallic contact surfaces such as piston and cylinder, SAE40-B30a demonstrated excessive wear and COF.

Because the ester compounds in WCB and the long chain polymers in PPO function as a ball bearing between rubbing surfaces, quaternary fuels operate as a friction-resisting agent in the lubricant sample, forming a protective layer between the metallic contact. As a consequence of the chemical interaction of fuel on the steel ball surface to preserve the rubbing surface, PPO based quaternary fuel in lubricant demonstrated polishing wear. PPO and WCB in B10 were shown to be viable alternative fuels because they demonstrated reduced lubricant degradation.

Declaration of Competing Interest

The authors declare that they have no known competing financial interests or personal relationships that could have appeared to influence the work reported in this paper.

Acknowledgements

The authors take the opportunity to thank the Universiti Malaya for the financial support under research grant IIRG008B-2019 under Universiti Malaya Impact-Oriented Interdisciplinary Research Grant Programme.

Appendix. Uncertainty analysis

(a) Coefficient of friction (COF)

Samples	COF 1	COF 2	COF 3	Min. D	Max. E	Accuracy (± 0.001)		Average H = (F + G)/2	Uncertainty (%)	
						Max. +0.001	Min. -0.001		+	-
						F	G		I = ((F-H)/H) * 100	I = ((G-H)/H) * 100
A	B	C	D	E	F	G	H = (F + G)/2	I = ((F-H)/H) * 100	I = ((G-H)/H) * 100	
SAE40	0.150	0.145	0.147	0.145	0.150	0.151	0.144	0.147	1.390	-1.390
SAE40-PB	0.172	0.164	0.168	0.164	0.172	0.173	0.163	0.168	2.262	-2.262
SAE40-PPO	0.150	0.152	0.167	0.150	0.167	0.168	0.149	0.159	5.300	-5.300
SAE40-WCB	0.149	0.154	0.145	0.145	0.154	0.155	0.144	0.150	2.941	-2.941
SAE40-B10	0.166	0.164	0.167	0.164	0.167	0.168	0.163	0.165	0.999	-0.999
SAE40-B20a	0.151	0.153	0.147	0.147	0.153	0.154	0.146	0.150	2.000	-2.000
SAE40-B30a	0.155	0.146	0.155	0.146	0.155	0.156	0.145	0.150	3.224	-3.224
SAE40-B3b	0.144	0.155	0.153	0.144	0.155	0.156	0.143	0.150	3.511	-3.511
SAE40-B40	0.150	0.152	0.151	0.150	0.152	0.153	0.149	0.151	0.595	-0.595
Average uncertainty of COF =									2.469	-2.469

(b) Wear scar diameter (WSD)

Samples	WSD 1 (μm)	WSD 2 (μm)	WSD 3 (μm)	Min. (μm)	Max. (μm)	Accuracy ($\pm 0.01 \mu\text{m}$)		Average (μm) H = (F + G)/2	Uncertainty (%)	
						Max. +0.01 μm	Min. -0.01 μm		+	-
						F	G		I = ((F-H)/H) * 100	I = ((G-H)/H) * 100
A	B	C	D	E	F	G	H = (F + G)/2	I = ((F-H)/H) * 100	I = ((G-H)/H) * 100	
SAE40	0.707	0.708	0.704	0.704	0.708	0.708	0.704	0.706	0.3	-0.3
SAE40-PB	0.812	0.820	0.811	0.811	0.820	0.820	0.811	0.816	0.5	-0.5
SAE40-PPO	0.688	0.679	0.674	0.674	0.688	0.688	0.674	0.681	1.0	-1.0
SAE40-WCB	0.630	0.622	0.620	0.620	0.630	0.630	0.620	0.681	0.8	-0.8
SAE40-B10	0.679	0.685	0.690	0.679	0.690	0.690	0.679	0.684	0.8	-0.8
SAE40-B20a	0.666	0.660	0.676	0.660	0.676	0.676	0.660	0.668	1.2	-1.2
SAE40-B30a	0.664	0.654	0.671	0.654	0.671	0.671	0.654	0.662	1.3	-1.3
SAE40-B3b	0.630	0.642	0.624	0.624	0.642	0.642	0.624	0.633	1.4	-1.4
SAE40-B40	0.598	0.600	0.582	0.582	0.600	0.600	0.582	0.591	1.5	-1.5
Average uncertainty of WSD =									1.0	-1.0

(c) Overall experimental uncertainty

$$\begin{aligned} \text{Overall experimental uncertainty} &= \text{square root of } [(\text{uncertainty of COF})^2 + (\text{uncertainty of WSD})^2] \\ &= \text{square root of } [(2.47)^2 + (1.00)^2] \\ &= \pm 2.66\% \end{aligned}$$

References

- [1] M. Gul, N.W.W. Zulkifli, H.H. Masjuki, M.A. Kalam, M.A. Mujtaba, M.H. Harith, A.Z. Syahir, W. Ahmed, A.B. Farooq, Effect of TMP-based-cottonseed oil-biolubricant blends on tribological behavior of cylinder liner-piston ring combinations, *Fuel* 278 (2020) 1118242.
- [2] M.A. Mujtaba, M.A. Kalam, H.H. Masjuki, M.E.M. Soudagar, H.M. Khan, H. Fayaz, M. Farooq, M. Gul, W. Ahmed, M. Ahmad, M. Munir, H. Yaqoob, O.D. Samuel, L. Razzaq, Effect of palm-sesame biodiesel fuels with alcoholic and nanoparticle additives on tribological characteristics of lubricating oil by four ball tribo-tester, *Alexandria Eng. J.* 60 (5) (2021) 4537–4546.
- [3] O. Elisha, A. Fauzi, E. Angraini, Analysis of Production and Consumption of Palm-Oil Based Biofuel using System Dynamics Model: Case of Indonesia, *Int. J. Sci. Eng. Technol.* 6 (2019).
- [4] M.A. Mujtaba, H. Muk Cho, H.H. Masjuki, M.A. Kalam, H.C. Ong, M. Gul, M.H. Harith, M.N.A.M. Yusoff, Critical review on sesame seed oil and its methyl ester on cold flow and oxidation stability, *Energy Rep.* 6 (2020) 40–54.
- [5] R. Latiff, in: H. Sarkar (Ed.), Malaysia to implement B30 biodiesel mandate intranport sector before 2025, REUTERS, Putrajaya, Malaysia, 2020.
- [6] O.M. Ali, R. Mamat, N.R. Abdullah, A.A. Abdullah, Analysis of blended fuel properties and engine performance with palm biodiesel–diesel blended fuel, *Renewable Energy* 86 (2016) 59–67.
- [7] C. Kaewbuddee, E. Sukjit, J. Srisertpol, S. Maithomklang, K. Wathakit, N. Klinkaew, P. Liplap, W. Arjharn, Evaluation of Waste Plastic Oil-Biodiesel Blends as Alternative Fuels for Diesel Engines, *Energies* 13 (11) (2020) 2823.
- [8] B. Sachuthananthan, D. Reddy, C. Mahesh, B. Dineshwar, Production of diesel like fuel from municipal solid waste plastics for using in CI engine to study the combustion, performance and emission characteristics, *Int. J. Pure Appl. Math.* 119 (2018) 85–96.
- [9] R.K. Singh, B. Ruj, A.K. Sadhukhan, P. Gupta, V.P. Tigga, Waste plastic to pyrolytic oil and its utilization in CI engine: Performance analysis and combustion characteristics, *Fuel* 262 (2020) 116539.
- [10] R. Kumar, M.K. Mishra, S.K. Singh, A. Kumar, Experimental evaluation of waste plastic oil and its blends on a single cylinder diesel engine, *J. Mech. Sci. Technol.* 30 (10) (2016) 4781–4789.
- [11] I. Kalargaris, G. Tian, S. Gu, Experimental evaluation of a diesel engine fuelled by pyrolysis oils produced from low-density polyethylene and ethylene–vinyl acetate plastics, *Fuel Process. Technol.* 161 (2017) 125–131.
- [12] K.A. Abed, A.K. El Morsi, M.M. Sayed, A.A.E. Shaib, M.S. Gad, Effect of waste cooking-oil biodiesel on performance and exhaust emissions of a diesel engine, *Egypt. J. Pet.* 27 (4) (2018) 985–989.
- [13] M. Gad, O.S. Abu-Elyazeed, M.A. Mohamed, A.M. Hashim, Effect of oil blends derived from catalytic pyrolysis of waste cooking oil on diesel engine performance, emissions and combustion characteristics, *Energy* 223 (2021) 120019.
- [14] M.F. Al-Dawody, A.A. Jazie, H. Abdulkadhim Abbas, Experimental and simulation study for the effect of waste cooking oil methyl ester blended with diesel fuel on the performance and emissions of diesel engine, *Alexandria Eng. J.* 58 (1) (2019) 9–17.
- [15] S.C. Sekhar, K. Karuppasamy, N. Vedaraman, A.E. Kabeel, R. Sathyamurthy, M. Elkelawy, H.A.E. Bastawissi, Biodiesel production process optimization from *Pithecellobium dulce* seed oil: Performance, combustion, and emission analysis on compression ignition engine fuelled with diesel/biodiesel blends, *Energy Convers. Manage.* 161 (2018) 141–154.
- [16] S.C. Sekhar, K. Karuppasamy, R. Sathyamurthy, M. Elkelawy, H.A.E.D. Bastawissi, P. Paramasivan, K. Sathiyamoorthy, P. Edison, Emission analysis on CI engine fuelled with lower concentrations of *Pithecellobium dulce* biodiesel–diesel blends, *Heat Transfer-Asian Res.* 48 (1) (2019) 254–269.
- [17] K.V. Yatish, H.S. Lalithamba, R. Suresh, H.R.H. Hebbar, Optimization of *bauhinia variegata* biodiesel production and its performance, combustion and emission study on diesel engine, *Renewable Energy* 122 (2018) 561–575.
- [18] M. Elkelawy, E.A. El Shenawy, H. Panchal, A. Elbanna, H.A. Bastawissi, K.K. Sadasivuni, Experimental investigation on the influences of acetone organic compound additives into the diesel/biodiesel mixture in CI engine, *Sustainable Energy Technol. Assess.* 37 (2020) 100614.
- [19] M. Elkelawy, H.A.E. Bastawissi, E.A. El Shenawy, M. Taha, H. Panchal, K.K. Sadasivuni, Study of performance, combustion, and emissions parameters of DI-diesel engine fuelled with algae biodiesel/diesel/n-pentane blends, *Energy Convers. Manage.: X* 10 (2021) 100058.
- [20] T. Ganapathy, R.P. Gakkhar, K. Murugesan, Optimization of performance parameters of diesel engine with *Jatropha* biodiesel using response surface methodology, *Int. J. Sustain. Energy.* 30 (1) (2011) S76–S90.
- [21] M. Elkelawy, H.A.E. Bastawissi, K.K. Esmaeil, A.M. Radwan, H. Panchal, K.K. Sadasivuni, M. Suresh, M. Israr, Maximization of biodiesel production from sunflower and soybean oils and prediction of diesel engine performance and emission characteristics through response surface methodology, *Fuel* 266 (2020) 117072.
- [22] A. Abu-Jrai, J.A. Yamin, A.H. Al-Muhtaseb, M.A. Hararah, Combustion characteristics and engine emissions of a diesel engine fuelled with diesel and treated waste cooking oil blends, *Chem. Eng. J.* 172 (1) (2011) 129–136.
- [23] H. An, W.M. Yang, A. Maghbouli, J. Li, S.K. Chou, K.J. Chua, Performance, combustion and emission characteristics of biodiesel derived from waste cooking oils, *Appl. Energy* 112 (2013) 493–499.
- [24] J. Taha-Tijerina, S. Shaji, S. Sharma Kanakillam, M.I. Mendivil Palma, K. Aviña, Tribological and thermal transport of Ag-vegetable nanofluids prepared by laser ablation, *Appl. Sci.* 10 (5) (2020) 1779, <https://doi.org/10.3390/app10051779>.
- [25] A.K. Agarwal, Lubricating oil tribology of a biodiesel-fuelled compression ignition engine, *Proceedings of the Spring Technical Conference of the ASME Internal Combustion Engine Division*, 2003.
- [26] A. Dhar, A.K. Agarwal, Experimental investigations of effect of Karanja biodiesel on tribological properties of lubricating oil in a compression ignition engine, *Fuel* 130 (2014) 112–119.
- [27] Y. Singh et al, Sustainability of Moringa-oil–based biodiesel blended lubricant, *Energy Sources Part A* 39 (3) (2017) 313–319.
- [28] M.A. Maleque, H.H. Masjuki, A.S.M.A. Haseeb, Effect of mechanical factors on tribological properties of palm oil methyl ester blended lubricant, *Wear* 239 (1) (2000) 117–125.
- [29] M.W. Sulek, A. Kulczycki, A. Malysa, Assessment of lubricity of compositions of fuel oil with biocomponents derived from rape-seed, *Wear* 268 (1-2) (2010) 104–108.
- [30] H.H. Masjuki, M.A. Maleque, Investigation of the anti-wear characteristics of palm oil methyl ester using a four-ball tribometer test, *Wear* 206 (1-2) (1997) 179–186.

- [31] M.S.N. Awang, N.W. Mohd Zulkifli, M.M. Abbas, S. Amzar Zulkifli, M.A. Kalam, M.H. Ahmad, M.N.A. Mohd Yusoff, M. Mazlan, W.M.A.W. Daud, Effect of Addition of Palm Oil Biodiesel in Waste Plastic Oil on Diesel Engine Performance, Emission, and Lubricity, *ACS Omega* 6 (33) (2021) 21655–21675.
- [32] S. Arumugam, G. Sriram, Preliminary Study of Nano- and Microscale TiO₂ Additives on Tribological Behavior of Chemically Modified Rapeseed Oil, *Tribol. Trans.* 56 (5) (2013) 797–805.
- [33] M.S. Awang, N.W. Zulkifli, M.M. Abbas, M.M. Zulkifli, S.A. Yusoff, M.H. Ahmad, M.A.H.L. Nohakim, W.M.A.W. Daud, Effect of addition of plastic pyrolytic oil and waste cooking oil biodiesel in palm oil biodiesel–commercial diesel blends on diesel engine performance, emission, and lubricity, *Energy Environ* (2021) 0958305X211034822.
- [34] A. Mujtaba, H.H. Masjuki, M.A. Kalam, F. Noor, M. Farooq, H.C. Ong, M. Gul, M.E. Soudagar, S. Bashir, I.M. Rizwanul Fattah, L. Razzaq, Effect of Additivized Biodiesel Blends on Diesel Engine Performance, Emission, Tribological Characteristics, and Lubricant Tribology, *Energies* 13 (2020) 3375.
- [35] H. Juwono, A. Singla, A. Kumar, D. Kumar, Catalytic conversion of Al-MCM-41-ceramic on hydrocarbon (C8 – C12) liquid fuel synthesis from polypropylene plastic waste, *AIP Conference Proceedings* (2018) 2049, 020080.
- [36] M.A. Mujtaba, H.H. Masjuki, M.A. Kalam, F. Noor, M. Farooq, H.C. Ong, M. Gul, M.E.M. Soudagar, S. Bashir, I.M. Rizwanul Fattah, L. Razzaq, Effect of Additivized Biodiesel Blends on Diesel Engine Performance, Emission, Tribological Characteristics, and Lubricant Tribology, *Energies* 13 (13) (2020) 3375.
- [37] S. Arumugam, G. Sriram, Effect of Bio-Lubricant and Biodiesel-Contaminated Lubricant on Tribological Behavior of Cylinder Liner-Piston Ring Combination, *Tribol. Trans.* 55 (4) (2012) 438–445.
- [38] Y. Singh, A. Singla, A. Kumar, D. Kumar, Friction and wear characteristics of jatropha oil-based biodiesel blended lubricant at different loads, *Energy Sources Part A* 38 (18) (2016) 2749–2755.
- [39] K. Nishimura, M. Miura, T. Hashimoto, K. Yari, M. Maruyama, N. Iseya, K. Takeoka, K. Yasuda, T. Yamazaki, Impacts on Engine Oil Performance by the Use of Waste Cooking Oil as Diesel Fuel, *SAE Technical Paper*, 2011.
- [40] M.A. Fazal, A.S.M.A. Haseeb, H.H. Masjuki, Investigation of friction and wear characteristics of palm biodiesel, *Energy Convers. Manage.* 67 (2013) 251–256.
- [41] M.S.N. Awang, N.W.M. Zulkifli, M.M. Abbass, M.S. Zulkifli, M.N.A.M. Yusoff, M.H. Ahmad, W.M.A.W. Daud, Effect of blending local plastic pyrolytic oil with diesel fuel on lubricity, *Jurnal Tribologi* 27 (2020) 143–157.
- [42] R.R. Sahoo, S.K. Biswas, Frictional response of fatty acids on steel, *J. Colloid Interface Sci.* 333 (2) (2009) 707–718.
- [43] A.C.M.d. Farias, J.T.N.d. Medeiros, S.M. Alves, Micro and nanometric wear evaluation of metal discs used on determination of biodiesel fuel lubricity, *Mater. Res.* 17 (1) (2014) 89–99.
- [44] G. Knothe, Dependence of biodiesel fuel properties on the structure of fatty acid alkyl esters, *Fuel Process. Technol.* 86 (10) (2005) 1059–1070.
- [45] D.P. Geller, J.W. Goodrum, Effects of specific fatty acid methyl esters on diesel fuel lubricity, *Fuel* 83 (17-18) (2004) 2351–2356.